

Synthesis and Stereochemistry of *N*-Phenyl-*N*-9-triptycylhydroxylamine Derivatives and Related Compounds

Chiharu Agawa, Keiko Otsuka, Mao Minoura, Yasuhiro Mazaki, and Gaku Yamamoto*

Department of Chemistry, School of Science, Kitasato University, Kitasato, Sagami-hara, Kanagawa 228-8555

Received July 30, 2004; E-mail: gyama@kitasato-u.ac.jp

During the course of attempts at synthesis of *N*-phenyl-*N*-9-triptycylhydroxylamine (**1**), we found that the reaction of *N*-9-triptycylhydroxylamine (**5**) with benzenediazonium-2-carboxylate afforded 3-(2-carboxyphenyl)-1-(9-triptycyl)triazene 1-oxide (**6**), the structure of which was confirmed by X-ray crystallography. Oxidation of *N*-(9-triptycyl)aniline (**4**) with *m*CPBA gave phenyl 9-triptycyl nitroxide (**7**) and *N*-(9-triptycyl)-1,4-benzoquinonimine (**8**) in small yields. Reduction of **7** with phenylhydrazine gave **1**, and *O*-ethylation of **1** gave *O*-ethyl-*N*-phenyl-*N*-9-triptycylhydroxylamine (**2**). Results of X-ray crystallography for compounds **2**, **4**, **7**, and **8** and results of dynamic NMR studies for **1**, **2**, and **8** are presented. In compound **8**, Tp–N rotation and C=N topomerization took place on the NMR timescale at high temperatures above 60 °C, and the energy barriers to both processes were obtained. In compounds **1** and **2**, dynamic NMR behavior was observed at very low temperatures below ca. –50 °C, and the energy barriers to the respective processes could not be determined except for those related to “Ph-passing”.

We have hitherto reported on the static and dynamic stereochemistry of various triptycene derivatives carrying a nitrogen atom at the bridgehead, such as *N,N*-dialkyl-9-triptycylamines,^{1,2} *N*-(9-triptycyl)anilines,^{3,4} *N*-(9-triptycyl)acetamides,^{5–7} and *N*-(9-triptycyl)acetanilide.⁸ We have recently been interested in *N*-9-triptycylhydroxylamines and have reported on the molecular structures in crystal and the dynamic behavior in solution of those carrying alkyl group(s) on the nitrogen or oxygen atom or on both.^{9–12} We naturally planned to study the corresponding *N*-aryl derivatives of the hydroxylamine, because significantly different behavior has often been observed between the *N*-alkyl and *N*-aryl derivatives of the above-mentioned compounds. We have thus made various attempts at syntheses of *N*-phenyl-*N*-9-triptycylhydroxylamine (**1**) and its *O*-alkyl derivatives (Chart 1). After several unsuccessful attempts, compound **1** and its *O*-ethyl derivative **2** could be obtained, and the dynamic NMR studies on these compounds will be described in this article. We found some interesting chemistry during the course of these studies, which will also be reported.

At the outset, we attempted reactions of organometallic compounds with nitroso compounds, because such reactions have been known to be the typical preparation methods of hydroxylamines. Reaction of phenyllithium with 9-nitrosotriptycene resulted in the formation of *O*-phenyl-*N*-9-triptycylhydroxylamine (**3**), instead of the desired *N*-phenyl derivative **1**, presumably by way of the single electron transfer process, which has been reported previously.⁹

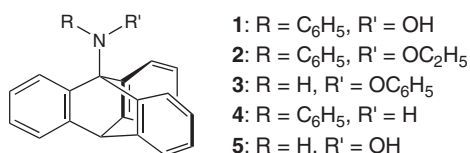


Chart 1.

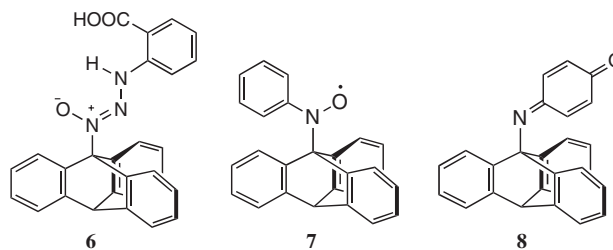


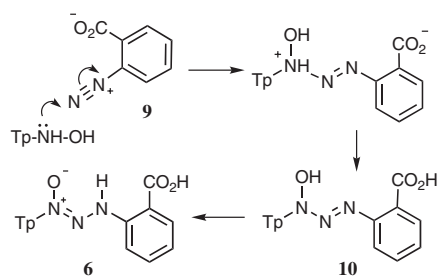
Chart 2.

Since it had been established that benzyne reacted with 9-triptycylamine to give *N*-(9-triptycyl)aniline (**4**)⁴ by N–H insertion of the benzyne, thermal decomposition of benzenediazonium-2-carboxylate, a well-known precursor of benzyne, in the presence of *N*-9-triptycylhydroxylamine (**5**) was examined. We expected the addition of benzyne to the NHOH moiety, but the product was found to be 3-(2-carboxyphenyl)-1-(9-triptycyl)triazene 1-oxide (**6**), a direct addition product of benzenediazonium-2-carboxylate with **5** as described below (Chart 2).

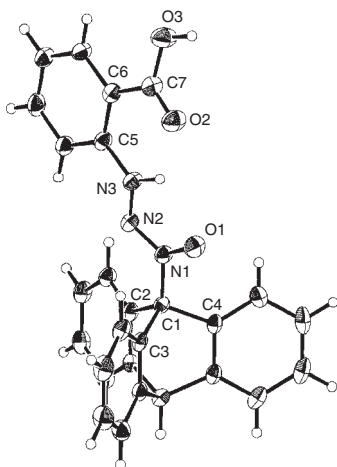
Then we attempted the oxidation of *N*-(9-triptycyl)aniline (**4**) to give *N*-phenyl-*N*-9-triptycylhydroxylamine (**1**). Oxidation with *m*CPBA was thus examined, but the reaction afforded only a small amount (ca. 7%) of phenyl 9-triptycyl nitroxide (**7**), together with *N*-(9-triptycyl)-1,4-benzoquinonimine (**8**), also in a similar small yield. An *N*-alkyl-1,4-benzoquinonimine is rather a rare type of molecule and the molecular structure and dynamic behavior of **8** was investigated in detail. Reduction of the nitroxide **7** gave the hydroxylamine **1** and ethylation of **1** gave the *O*-ethyl derivative **2**. Dynamic NMR studies of these compounds are described below.

Results and Discussion

Reaction of Benzenediazonium-2-carboxylate with *N*-9-Triptycylhydroxylamine. Benzenediazonium-2-carboxylate



Scheme 1.

Fig. 1. The ORTEP drawing with 50% probability ellipsoids of compound **6**.

(**9**),¹³ prepared by aprotic diazotization of anthranilic acid, was heated in boiling chloroform in the presence of *N*-9-triptycylhydroxylamine (**5**) to afford a white solid mass in a high yield, which was finally identified to be 3-(2-carboxyphenyl)-1-(9-triptycyl)triazene 1-oxide (**6**). Mass spectral analysis suggested the product to be a 1:1 adduct of **9** with **5**. Although IR and NMR spectra could not definitely differentiate **6** from the tautomeric hydroxytriazene **10** (Scheme 1), X-ray crystallographic analysis confirmed the structure of **6**.

The molecular structure of **6** is shown in Fig. 1. Selected lengths and angles are given in the Experimental Section. The triazene oxide moiety is almost coplanar with the *o*-carboxyphenyl group (N2–N3–C5–C6: -168.5°) and nearly eclipses one of the benzene rings of the Tp moiety (N2–N1–C1–C2: 20.0°). The NH moiety intramolecularly hydrogen bonds both with the *N*-oxide oxygen and the carbonyl oxygen (O1...N3: 2.473 Å; O2...N3: 2.653 Å). This will be coincident with the appearance of the NH proton at a very low field (δ 13.5) in the ¹H NMR spectrum. Two molecules of **6** associate to form a hydrogen-bonded dimer by way of the carboxy groups.

A plausible mechanism of formation of **6** is given in Scheme 1.

At first, the facile reaction of benzenediazonium-2-carboxylate (**9**) with the hydroxylamine **5** before decomposing to benzyne seemed surprising, because the corresponding amine, TpNH₂, does not react with **9** but with benzyne formed by decomposition of **9** and gives **4** in a good yield.⁴ This indicates that TpNHOH has far stronger nucleophilicity than TpNH₂,

although amines are generally far more basic than the corresponding hydroxylamines: the p*K*_b values have been reported to be 8.03, 8.04, 8.80, 9.40, 9.25, and 10.35 for NH₂OH, MeNHOH, Me₂NOH, NH₂OMe, MeNHOME, and Me₂NOMe, respectively,¹⁴ and 4.75, 3.38, 3.23, and 4.20 for NH₃, MeNH₂, Me₂NH, and Me₃N, respectively.¹⁵ A literature survey revealed that the above-mentioned type of reaction is not unprecedented: *N*-phenylhydroxylamine, for example, reacted with diazotized anthranilic acid to give 3-(2-carboxyphenyl)-1-phenyltriazene 1-oxide,¹⁶ the structure of which was confirmed by X-ray crystallography.¹⁷

Oxidation of *N*-(9-Triptycyl)aniline with *m*-Chloroperbenzoic Acid. Oxidation of secondary amines to the corresponding hydroxylamines or nitroxides has sporadically been reported; many of the researchers used *m*-chloroperbenzoic acid (*m*CPBA) as the oxidant. Therefore, oxidation of **4** with *m*CPBA was examined, which proved to give phenyl 9-triptycyl nitroxide (**7**) together with *N*-(9-triptycyl)-1,4-benzoquinonimine (**8**), both in small amounts.

The nitroxide **7** has been reported as the spin-trap product of phenyl radical with 9-nitrosotriptycene,¹⁸ where only the ESR data were given without further characterization. The ESR data found in our compound **7** agreed well with those reported in Ref. 18. X-ray crystallographic analysis of **7** was performed in order to confirm the structure: the molecular structure is shown in Fig. 2(a) and the representative bond lengths and angles are given in Table 1. The phenyl ring is nearly coplanar with the Tp–N bond and almost bisects the notch between two benzene rings of the Tp group. The nitrogen is slightly pyramidalized: the sum of the bond angles around the nitrogen is 358.0° . This is contrasted with the complete planarity of the nitroxide moieties found recently in an alkyl aryl nitroxide¹⁹ and a dialkyl nitroxide,²⁰ and can be ascribed to the steric effect of the bulky Tp moiety.

Reduction of the nitroxide **7** with phenylhydrazine gave *N*-phenyl-*N*-9-triptycylhydroxylamine (**1**) almost quantitatively as shown by NMR, the isolation yield being 83%. Compound **1** was rather unstable and easily oxidized to **7** in the air. Deprotonation of **1** with potassium *t*-butoxide followed by treatment with ethyl iodide gave *O*-ethyl-*N*-phenyl-*N*-9-triptycylhydroxylamine (**2**). X-ray crystallographic and dynamic NMR studies on this compound will be described in a later section.

The molecular structure of *N*-(9-triptycyl)-1,4-benzoquinonimine (**8**), the other oxidation product of compound **4**, is shown in Fig. 2(b) together with that of **4** in Fig. 2(c) for comparison. The representative bond lengths and angles are also compiled in Table 1. The quinone ring in **8** or the phenyl ring in **4** is coplanar with the Tp–N bond and almost bisects the notch of the Tp moiety.

Dynamic NMR Studies of the Quinonimine 8. Compound **8** shows an interesting stereochemical behavior in solution in the sense that two types of dynamic processes are possible: rotation about the Tp–N bond and topomerization of the C=N double bond. Actually these two processes were observed by NMR spectroscopy in different temperature ranges. At room temperature, both processes are slow on the NMR timescale: one of the Tp-benzene ring is different from the other two and two edges of the quinone ring are mutually non-equivalent. As the temperature of the sample in 1,1,2,2-tetra-

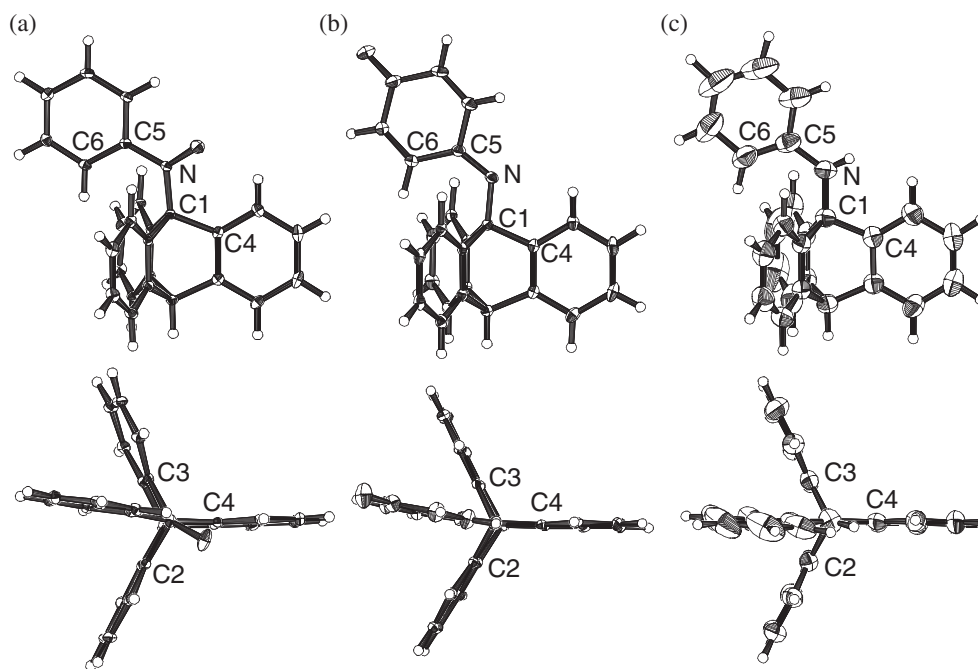


Fig. 2. The ORTEP drawings with 50% probability ellipsoids of (a) compound **7**, (b) compound **8**, and (c) compound **4**.

Table 1. Selected Bond Lengths (Å) and Angles (°) for Compounds **7**, **8**, and **4**^{a)}

Compound	7	8	4
N–C5	1.434(2)	1.298(2)	1.398(3)
N–C1	1.488(2)	1.459(2)	1.444(3)
C1–C2	1.553(2)	1.552(2)	1.540(3)
C1–C3	1.552(2)	1.551(2)	1.541(3)
C1–C4	1.554(2)	1.546(2)	1.531(3)
C1–N–C5	122.8(1)	123.6(2)	126.4(2)
O–N–C5	117.4(1)	—	—
O–N–C1	117.8(1)	—	—
N–C1–C2	109.7(1)	114.8(2)	114.8(2)
N–C1–C3	114.0(1)	117.2(2)	114.6(2)
N–C1–C4	116.2(2)	109.2(1)	112.0(2)
C1–N–C5–C6	7.4(2)	−0.8(2)	−8.7(4)
C5–N–C1–C2	−72.6(1)	−67.6(2)	−59.1(3)
C5–N–C1–C3	50.2(1)	57.8(2)	65.5(3)
C5–N–C1–C4	168.8(1)	175.0(2)	−176.7(2)

a) The atom numbering is shown in Fig. 2.

chloroethane-*d*₂ was raised, the Tp-aromatic signals began broadening at ca. 60 °C and coalesced above 90 °C, while the quinone ring signals began broadening only above 110 °C. The aromatic region spectra of **8** at several temperatures are shown in Fig. 3.

The lineshape change of the Tp-aromatic signals is ascribed to the rotation of the Tp–N bond, and lineshape analysis of the signals due to 4-, 5-, and 16-H at six temperature points in the range of 80–100 °C gave the rate constant at each temperature. In addition, saturation transfer experiments were performed by observing the intensity change of the 13-H signal (δ 8.12) upon irradiation of the 1,8-H signal (δ 6.88) to afford rate constants at five temperature points in the range of 39–59 °C. Least

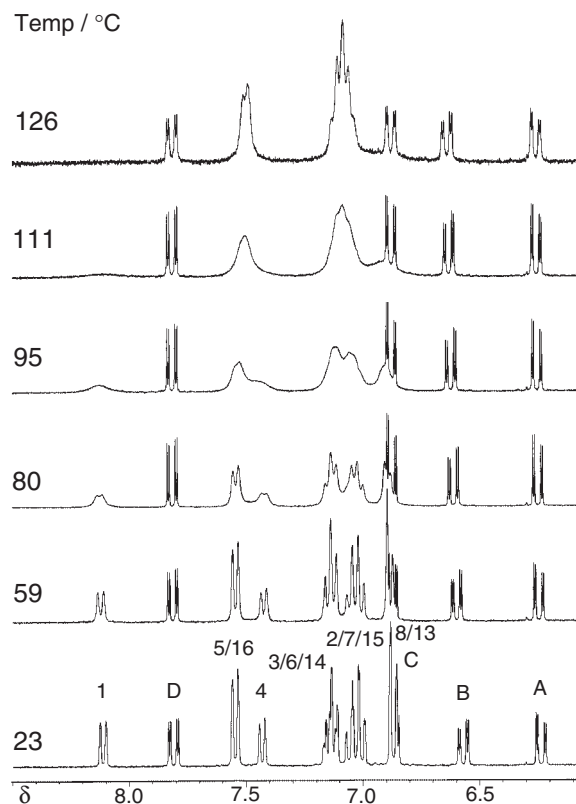
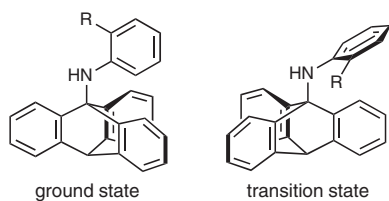
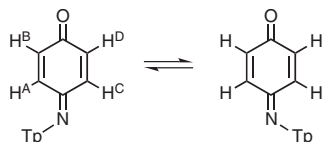


Fig. 3. ¹H NMR spectra of compound **8** in the aromatic region at several temperatures in 1,1,2,2-tetrachloroethane-*d*₂.

squares analysis of the Eyring plot including the whole temperature range gave the following kinetic parameters: $\Delta H^\ddagger = 74.4 \pm 1.3$ kJ mol^{−1}, $\Delta S^\ddagger = -14.4 \pm 3.9$ J mol^{−1} K^{−1}, ΔG^\ddagger (80 °C) = 79.5 kJ mol^{−1}. This is the highest energy barrier



Scheme 2.



Scheme 3.

to rotation of the Tp–N bond hitherto known. The ΔG^\ddagger values for the Tp–N rotation so far reported are, for example, 45.6 kJ mol⁻¹ (–59 °C) in *N*-(9-triptycyl)aniline (**4**)⁴ and 70.2 kJ mol⁻¹ (26 °C) in *N*-2-biphenyl-9-triptycylamine (**11**).⁴ These compounds at the ground state adopt a conformation in which the aryl or quinone ring is almost coplanar with the Tp–N bond (Scheme 2), as revealed by the molecular structures in crystal (see Fig. 2). At the transition state for the Tp–N rotation, the aryl or quinone plane should significantly twist in order to relieve the steric repulsion against the Tp moiety. Compound **4** can easily adopt such a conformation as shown in Scheme 2 at the transition state (R = H), while compound **11** (R = C₆H₅) is subject to significant steric congestion even in a twisted conformation at the transition state, and this causes the barrier in **11** to be far higher than that in **4**. Compound **8** finds it even harder to adopt a twisted conformation similar to the one shown in Scheme 2 at the transition state because the nitrogen constitutes a double bond, and thus the barrier is even higher.

The second dynamic process of **8** observed at higher temperatures is the topomerization of the C=N double bond (Scheme 3). Because coalescence of the quinone-ring protons could not be expected below the boiling point of the solvent used (145 °C), lineshape analysis was abandoned, and the rate constants for this process were obtained by saturation transfer experiments at four temperature points in the range of 110–125 °C. Here the change in the signal intensity of H^D (δ 7.81, see Fig. 3 and Scheme 3) was followed upon irradiation of H^B (δ 6.57). Least squares analysis of the Eyring plot gave the following kinetic parameters: $\Delta H^\ddagger = 86.2 \pm 4.5$ kJ mol⁻¹, $\Delta S^\ddagger = -22.3 \pm 11.5$ J mol⁻¹ K⁻¹, ΔG^\ddagger (126 °C) = 95.1 kJ mol⁻¹.

A lot of studies have been reported on the isomerization or topomerization of C=N double bonds.²¹ The isomerization/topomerization can take place either by rotation around the C=N bond or planar inversion at the nitrogen atom, and theoretical studies have indicated that the latter generally has a lower energy barrier than the former. Therefore, planar inversion is tentatively assigned to the observed process. The ΔG^\ddagger values have been reported to be 102.5 and 92.0 kJ mol⁻¹ for the C=N bond topomerization in compounds **12**²² and **13**,²³ respectively (Chart 3).

X-ray Crystallography of Compound 2. A single crystal

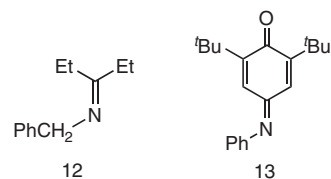


Chart 3.

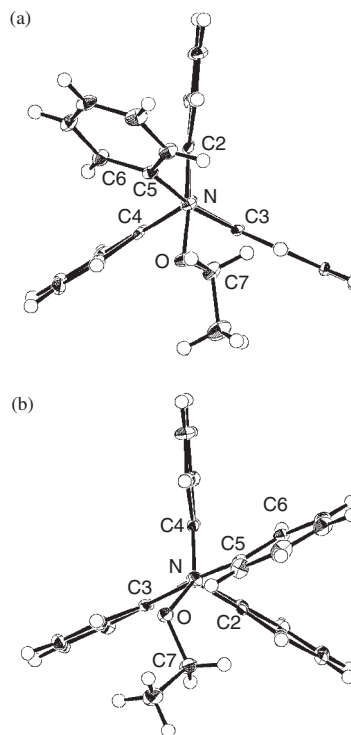


Fig. 4. The ORTEP drawings with 50% probability ellipsoids of (a) molecule **A** and (b) molecule **B** of compound **2**.

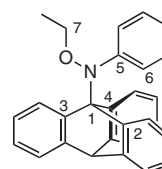


Chart 4.

of compound **2** contained two kinds of molecules in a crystal lattice; these are referred to as molecules **A** and **B**. Perspective drawings of these molecules are shown in Fig. 4, and selected bond lengths, bond angles, and torsion angles are compiled in Table 2.

These two molecules have opposite chirality for the nitrogen and are significantly different in their conformations and geometries. The structure of molecule **A** is rather similar to the structures of the *N,O*-dialkyl-*N*-9-triptycylhydroxylamines hitherto reported.¹² The nitrogen has an almost tetrahedral geometry (the sum of the angles around nitrogen is 332.3°), and the C1–N–O–C7 dihedral angle (149.3°) is characteristic of an *N*-9-triptycylhydroxylamine as discussed in detail previously (see Chart 4 for the atomic numbering).¹² This angle results

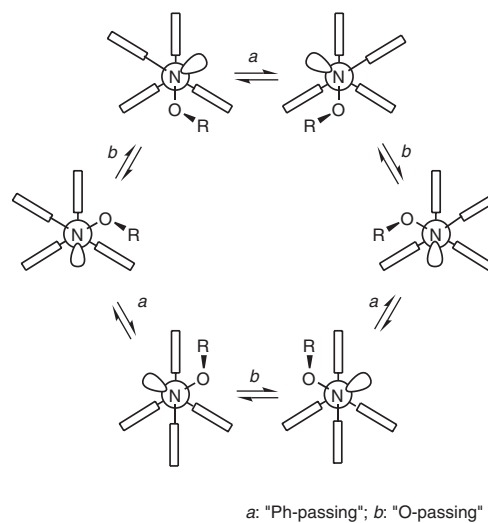
Table 2. Selected Bond Lengths (Å) and Angles (°) for the Two Molecules of Compound **2**^{a)}

Molecule	A	B
N–O	1.465(2)	1.404(2)
N–C1	1.466(2)	1.469(2)
C1–C2	1.552(2)	1.558(2)
C1–C3	1.546(2)	1.560(2)
C1–C4	1.554(2)	1.552(2)
N–C5	1.452(2)	1.407(2)
O–C7	1.439(2)	1.451(2)
C1–N–O	105.2(1)	117.5(1)
C1–N–C5	117.6(1)	124.1(1)
C5–N–O	109.5(1)	112.2(1)
Sum	332.3	353.8
N–C1–C2	112.2(1)	115.7(2)
N–C1–C3	110.3(1)	116.0(2)
N–C1–C4	118.3(1)	110.0(1)
N–O–C7	111.3(1)	114.1(1)
C1–N–O–C7	149.3(1)	77.6(2)
C5–N–O–C7	–83.4(2)	–75.8(2)
O–N–C1–C2	176.7(1)	–99.2(2)
O–N–C1–C3	–70.2(1)	25.3(2)
O–N–C1–C4	50.8(2)	139.5(1)
C5–N–C1–C2	54.5(2)	50.8(2)
C5–N–C1–C3	167.6(1)	175.3(2)
C5–N–C1–C4	–71.4(2)	–70.5(2)
C1–N–C5–C6	25.3(2)	12.8(2)
O–N–C5–C6	–94.7(2)	164.2(1)

a) The atom numbering is shown in Chart 4 and Fig. 4.

from the steric repulsion between the *O*-methylene group and the nearby benzene ring of the Tp moiety, which distorts the angle from the “ideal” value of 120°. The phenyl plane is tilted from the C1–N–C5 plane by ca. 25° because of the steric interaction with the *O*-methylene group, and is almost perpendicular to the O–N–C5 plane. In molecule **B**, on the contrary, the nitrogen is highly planarized (the sum of the angles around nitrogen is 353.8°), and the N–O and N–C5 bonds are not as long as those of molecule **A**. The phenyl plane is tilted from the C1–N–C5 and O–N–C5 planes to similar degrees (ca. 15°). One may reasonably infer that the nitrogen lone-pair conjugates with the phenyl group and thus diminishes the electrostatic repulsion with the oxygen lone-pairs, resulting in the shortening of both the N–C5 and N–O bonds. The C1–N–O–C7 dihedral angle is 77.6° and thus the O–C7 bond almost bisects the C1–N–C5 angle. In other words, the O–C7 bond is antiperiplanar to the nitrogen lone-pair, and this conformation corresponds to the second stable one in hydroxylamines (see Scheme 2 of Ref. 12). This is the first example of such a conformation found in crystal.

Dynamic NMR Study of Compounds 1 and 2. The plausible mechanistic pathway of conformer interconversion in *N*-phenyl-*N*-9-triptycylhydroxylamines, **1** and **2**, is schematically shown in Scheme 4 by the analogy of the *N*-alkyl derivatives discussed previously.¹² The molecule is assumed to reside in a conformation similar to molecule **A** in the crystal of **2**. Thus, one conformer transforms to its enantiomeric conformer by the passing of either the phenyl group or the OR group over a benzene ring of the Tp moiety (referred to as “Ph-passing”



Scheme 4.

or “O-passing”, respectively⁴). Each passing process is accompanied by inversion of the nitrogen and partial rotation of the N–O bond. In the “Ph-passing”, the phenyl group necessarily rotates by ca. 180° and thus the two edges interchange (so-called “Gear Rotation” or GR).⁴ The phenyl group can also rotate inside the notch made of the two flanking benzene rings, independently of the “Ph passing” process (so-called “Isolated Rotation” or IR).⁴

At room temperature, completely conformationally averaged NMR spectra were obtained for both compounds; the three benzene rings of the Tp moiety were mutually equivalent and the *N*-phenyl proton signals appeared as an A₂B₂C spin system. The methylene protons of the ethyl group in **2** gave a sharp quartet signal. Many of the signals broadened and de-coalesced with the decrease of the temperature, but completely re-sharpened spectra were not obtained even at the lowest temperatures examined (–100 °C and –115 °C for **1** and **2**, respectively). Spectra of the aromatic region at several temperatures are shown in Figs. 5 and 6 for **1** and **2**, respectively.

At the lowest temperatures, some of the signals could be assigned by decoupling and qualitative saturation transfer experiments, and the assignments are given in Figs. 5 and 6. In compound **1**, the edge-exchange of the phenyl group, i.e., the rotation of the N–Ph bond, was slow on the NMR timescale at –100 °C, and the two ortho-protons (2'- and 6'-H) were separately observed: the 2'-H signal appeared at a considerably high field of δ 6.32 because of the ring-current effect of the flanking benzene rings of the Tp moiety (Fig. 5). The chemical shift is similar to that of the 2'-H signal in compound **4** (δ 6.15 at –87 °C),⁴ indicating that the phenyl plane is almost coplanar with the C9–N–C1' plane (Chart 5). From the chemical shift difference between the 2'-H and 6'-H signals (ca. 350 Hz), the rate constant for the N–Ph rotation was roughly estimated to be ca. 780 s^{–1} at the plausible coalescence temperature (ca. –60 °C), corresponding to ΔG^\ddagger of ca. 40 kJ mol^{–1}. The N–Ph rotation takes place by two processes, GR (Ph-passing) and IR, as mentioned above, and thus the rate constant of ca. 780 s^{–1} is the sum of the rate constants for these two processes. This means that ΔG^\ddagger of both GR and IR should not be less than 40 kJ mol^{–1}.

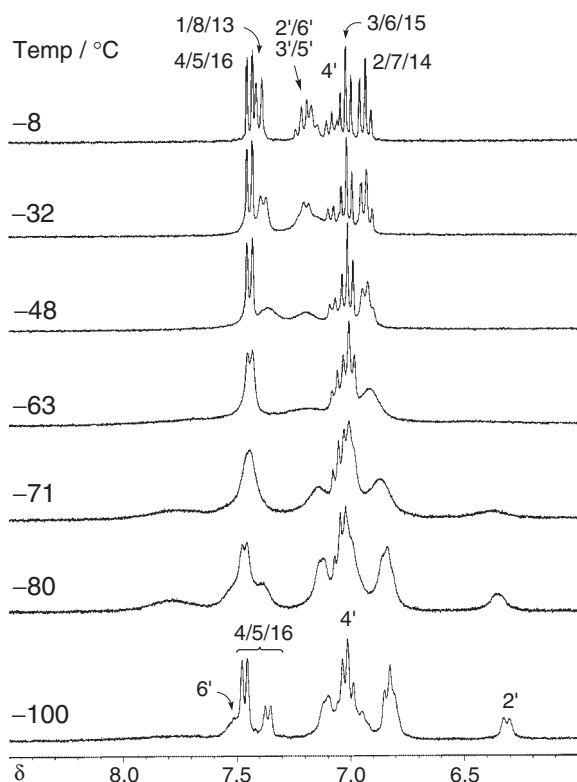


Fig. 5. ^1H NMR spectra of compound **1** in the aromatic region at several temperatures in dichloromethane- d_2 . The numberings are shown in Chart 5.

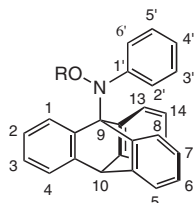


Chart 5.

As for the Tp-proton signals of **1**, those due to 4/5/16-H appeared as two doublets with the intensity ratio of 2:1 at -100 °C, and the other signals were obscure because of the signal broadening and overlapping (Fig. 5). As can be inferred from Scheme 4, three benzene rings of the Tp moiety are equivalent when both Ph-passing and O-passing are fast, and are mutually nonequivalent when both processes are slow, while two are equivalent and one is different when either one process is slow and the other is fast. The appearance of the 4/5/16-H signals at -100 °C corresponds to the last situation. The lineshape of the 4/5/16-H signal at -80 °C gave a rough estimate of the rate constant of ca. 25 s^{-1} and thus ΔG^\ddagger of ca. 41 kJ mol^{-1} for the site-exchange, which corresponds to the slower of the two processes. This means that both Ph-passing and O-passing have ΔG^\ddagger of ca. 41 kJ mol^{-1} or lower. From these results and those given in the preceding paragraph, ΔG^\ddagger of the Ph-passing process is concluded to lie between 40 and 41 kJ mol^{-1} , while the ΔG^\ddagger values of the IR and O-passing processes are not determined.

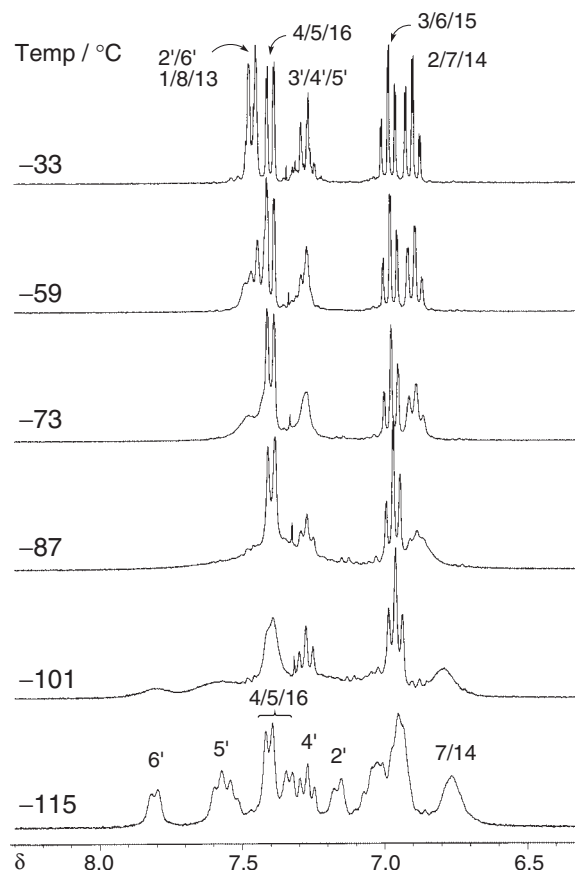


Fig. 6. ^1H NMR spectra of compound **2** in the aromatic region at several temperatures in dichloromethane- d_2 . The numberings are shown in Chart 5.

In compound **2**, the signals due to the phenyl group were separately identified at -115 °C except for 3'-H, indicating the slow rotation of the N-Ph bond (Fig. 6). The 2'-H signal appeared at δ 7.17, a considerably lower field than the corresponding signal in compound **1**, probably because of the tilting of the phenyl plane out of the C9-N-C1' plane. From the chemical shift difference between the 2'-H and 6'-H signals (ca. 195 Hz), the rate constant for the N-Ph rotation was roughly estimated to be ca. 430 s^{-1} at a plausible coalescence temperature (ca. -90 °C), corresponding to ΔG^\ddagger of ca. 35 kJ mol^{-1} . The signals due to the Tp moiety were still broad at -115 °C. The 4/5/16-H signals appeared as 2:1 doublets as did those in **1**, indicating that either Ph-passing or O-passing is slow but the other is fast at this temperature. A rough estimate of the rate constant of ca. 15 s^{-1} and ΔG^\ddagger of ca. 36 kJ mol^{-1} at -108 °C was obtained for the site exchange. The methylene signal remained a broad quartet at -115 °C, in agreement with the reasoning that either Ph-passing or O-passing is still fast at this temperature. By similar reasoning as in **1**, one can infer that ΔG^\ddagger of the Ph-passing process in **2** lies between 35 and 36 kJ mol^{-1} .

The results of the DNMR studies for **1** and **2** are given in Table 3, together with the data for the related compounds previously reported. Both the R-passing and O-passing barriers in **1** and **2** are considerably lower than the respective counterparts in *N*-methyl derivatives **14** and **15**. The lower barrier to R-

Table 3. The Results of DNMR Studies for **1**, **2**, and Related Compounds^{a)}

Compd	R	R ¹	$\Delta G^\ddagger/\text{kJ mol}^{-1}$			Ref
			R-passing	O-passing	IR	
1	Ph	OH	40–41	≤ 41	≥ 40	This work
2	Ph	OEt	35–36	≤ 36	≥ 35	This work
4	Ph	H	45.6	—	44.8	4
14	Me	OH	52.6	51.0	—	12
15	Me	OEt	57.7	46.5	—	12

a) Measured in dichloromethane-*d*₂.

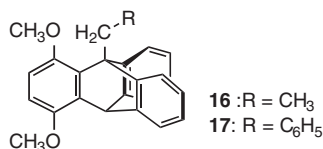


Chart 6.

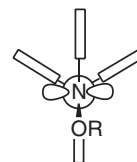


Chart 7.

passing in the *N*-phenyl compounds will be ascribed mainly to stabilization of the transition state by dynamic gearing (an analogy with that shown in Scheme 2). A similar situation was observed in 9-ethyl-1,4-dimethoxytryptcene (**16**) and its 9-benzyl counterpart **17**; the barrier to rotation of the 9-substituent was 61.1 kJ mol⁻¹ for **16** and 49.8 kJ mol⁻¹ for **17** (Chart 6).²⁴

It is notable that the GR (i.e., R-passing) barrier in **2** is lower than that in **1**, while that in **15** is higher than that in **14**. The latter has been discussed in terms of the steric interaction of the OR¹ moiety with the Tp group at the transition state, resulting in the higher barrier in **15** than in **14**.¹² The former would be ascribed mainly to the larger destabilization of the ground state in **2** than in **1** due to steric repulsion between the phenyl and the *O*-methylene groups.

The fact that the GR barrier is higher in **4** than in **1** or in **2** will again be mainly ascribed to ground state destabilization in **1** and **2**, though some other factors will contribute: the Ph plane in **4** is coplanar with the C1–N–C5 plane (see Fig. 2 for numbering), while that in **2** is considerably (ca. 25°) tilted as shown in Fig. 4(a).

The fact that the O-passing barriers in **1** and **2** are lower than in **14** and **15** probably results from the lower nitrogen inversion barrier in the *N*-phenyl compounds: the plausible transition state for O-passing in **1** and **2** will be stabilized by the phenyl group because of the conjugation with the nitrogen lone-pair (Chart 7).

Experimental

General. Melting points are not corrected. Mass spectra were obtained on a Hitachi M-2500 spectrometer in the EI mode. IR spectra were obtained on a Jasco FT/IR-610 spectrometer. ¹H and ¹³C NMR spectra were obtained on a Bruker ARX-300 spectrometer operating at 300.1 MHz for ¹H and 75.4 MHz for ¹³C, respectively, at 22–24 °C, unless otherwise stated. Chemical shifts are referenced with internal tetramethylsilane ($\delta_{\text{H}} = 0.00$) or CDCl₃ ($\delta_{\text{C}} = 77.00$). Letters p, s, t, and q given along with the ¹³C chemical shifts denote primary, secondary, tertiary, and quaternary, respectively. In variable-temperature experiments, temperatures were calibrated using a methanol sample or an ethylene

glycol sample and are reliable to ± 1 °C. The ESR spectrum of **7** was obtained on a JEOL JES-TE200 spectrometer.

3-(2-Carboxyphenyl)-1-(9-triptycyl)triazene 1-Oxide (6). To a boiling solution of 1.01 g (3.54 mmol) of *N*-9-triptycylhydroxylamine (**5**)²⁵ in 50 mL of chloroform was added during the course of 30 min a suspension in chloroform (30 mL) of benzenediazonium-2-carboxylate (**9**)¹³ prepared from 725 mg (5.29 mmol) of anthranilic acid, and the mixture was then heated under reflux for 30 min. The white precipitates formed were collected by filtration to afford 1.356 g (3.13 mmol, 88%) of **6**, mp 208–210 °C (from chloroform). Found: C, 74.81; H, 4.42; N, 9.69%. Calcd for C₂₇H₁₉N₃O₃: C, 74.81; H, 4.42; N, 9.69%. MS *m/z* 433 (M⁺). IR (KBr) 3400–2400 (br), 1678 (s) cm⁻¹. ¹H NMR (CDCl₃) δ 5.427 (1H, s, 10-H), 7.04–7.16 (7H, m, 2/7/14-H, 3/6/15-H, 4'-H), 7.442 (3H, m, 4/5/16-H), 7.615 (1H, dd, *J* = 8.6, 7.2, 1.6 Hz, 5'-H), 7.758 (1H, dd, *J* = 8.5, 0.9 Hz, 6'-H), 7.891 (3H, m, 1/8/13-H), 8.219 (1H, dd, *J* = 8.0, 1.4 Hz, 3'-H), 13.49 (1H, s, NH). The carboxy proton was not detected in CDCl₃ but was found at δ 8.31 in DMSO-*d*₆. ¹³C NMR (CDCl₃) δ 53.59 (1C, t), 84.28 (1C, q), 113.47 (1C, t), 114.37 (1C, t), 121.03 (1C, t), 122.97 (3C, t), 123.05 (3C, t), 124.94 (3C, t), 125.77 (3C, t), 131.70 (1C, q), 134.09 (1C, q), 141.71 (3C, q), 142.15 (1C, q), 143.84 (3C, q), 169.15 (1C, q).

***m*CPBA Oxidation of *N*-(9-Triptycyl)aniline.** To an ice-chilled solution of 500 mg (1.45 mmol) of *N*-(9-triptycyl)aniline (**4**)⁴ in 40 mL of dichloromethane under argon was added 500 mg (2.90 mmol) of *m*-chloroperbenzoic acid in 60 mL of dichloromethane. The mixture was stirred for 1 h at 0 °C and then for 1 h at room temperature. The solution was washed with aq. NaHCO₃, dried over MgSO₄ and evaporated. Column chromatography on silica gel with dichloromethane–hexane gave 32 mg (6%) of phenyl 9-triptycyl nitroxide (**7**) and 40 mg (7%) of *N*-(9-triptycyl)-1,4-benzoquinonimine (**8**) together with 205 mg (41%) of unreacted **4**.

Phenyl 9-Triptycyl Nitroxide (7). Reddish-brown solids, mp 236–244 °C (dec) (from dichloromethane–hexane). Found: C, 86.70; H, 4.99; N, 3.91%. Calcd for C₂₆H₁₈NO: C, 86.64; H, 5.03; N, 3.89%. MS *m/z* 360 (M⁺, 60%), 345 (85%), 252 (100%). ESR (CH₂Cl₂, 22 °C) *g* = 2.0074, *a* = 11.1 (t), 2.1 (q), and 0.9 (t) G (lit.¹⁸ *a* = 11.1, 2.2, and 0.9 G in benzene).

***N*-(9-Triptycyl)-1,4-benzoquinonimine (8).** Colorless crystals, mp 254–260 °C (dec) (from dichloromethane–hexane).

Found: C, 86.80; H, 4.81; N, 3.81%. Calcd for $C_{26}H_{17}NO$: C, 86.88; H, 4.77; N, 3.90%. 1H NMR ($CDCl_3$) δ 5.492 (1H, s, 10-H), 6.219 (1H, dd, $J = 10.4$, 2.3 Hz, 2'-H), 6.573 (1H, dd, $J = 10.4$, 2.7 Hz, 3'-H), 6.848 (2H, d, $J = 7.7$ Hz, 8/13-H), 6.852 (1H, dd, $J = 10.4$, 2.3 Hz, 6'-H), 6.967 (2H, td, $J = 7.5$, 1.3 Hz, 7/14-H), 6.992 (1H, td, $J = 7.0$, 1.3 Hz, 3-H), 7.080 (2H, td, $J = 7.3$, 1.2 Hz, 6/15-H), 7.087 (1H, td, $J = 7.5$, 1.3 Hz, 2-H), 7.376 (1H, dd, $J = 7.3$, 1.0 Hz, 4-H), 7.498 (2H, dd, $J = 7.3$, 1.1 Hz, 5/16-H), 7.777 (1H, $J = 10.1$, 2.7 Hz, 5'-H), 8.069 (1H, dd, $J = 7.5$, 1.2 Hz, 1-H). ^{13}C NMR ($CDCl_3$) δ 53.75 (1C, t, 10-C), 74.07 (1C, q, 9-C), 121.81 (2C, t), 122.30 (1C, t), 123.20 (1C, t), 124.01 (2C, t), 124.58 (2C, t), 125.09 (1C, t), 125.19 (1C, t), 126.01 (2C, t), 129.58 (1C, t), 131.76 (1C, t), 132.67 (1C, t), 143.69 (1C, t), 143.69 (2C, q), 144.28 (2C, q), 144.57 (1C, q), 147.34 (1C, q), 162.44 (1C, q, C=N), 187.71 (1C, q, C=O).

N-Phenyl-N-9-triptycylhydroxylamine (1). To a solution of 30 mg (0.083 mmol) of phenyl 9-triptycyl nitroxide (**7**) in 5 mL of dichloromethane was added 9 μ L (0.09 mmol) of phenylhydrazine, and the solution was stirred at room temperature for 5 min. Column chromatography on silica gel with dichloromethane–hexane (1:3) afforded 25 mg (0.069 mmol, 83%) of **1** as white solids, mp 223–224 °C (dec) (from dichloromethane–hexane). Found: C, 86.61; H, 5.45; N, 3.85%. Calcd for $C_{26}H_{19}NO$: C, 86.40; H, 5.30; N, 3.88%. 1H NMR ($CDCl_3$) δ 5.381 (1H, s, 10-H), 6.692 (1H, s, OH), 6.929 (3H, td, $J = 7.5$, 1.4 Hz, 2/7/14-H), 7.001 (3H, td, $J = 7.4$, 1.3 Hz, 3/6/15-H), 7.089 (1H, m, *p*-H), 7.20–7.26 (4H, m, *o*- and *m*-H), 7.413 (3H, dd, $J = 7.4$, 1.4 Hz, 4/5/16-H), 7.451 (3H, d, $J = 7.5$ Hz, 1/8/13-Hz). ^{13}C NMR ($CDCl_3$) δ 54.31 (1C, t), 76.17 (1C, q), 123.34 (3C, t), 123.76 (4C, t), 124.31 (3C, t), 125.04 (3C, t), 125.15 (3C, t), 127.52 (1C, t), 143.05 (3C, q), 145.33 (3C, q), 149.13 (1C, q).

O-Ethyl-N-phenyl-N-9-triptycylhydroxylamine (2). To an ice-chilled solution of 45 mg (0.124 mmol) of **1** in 8 mL of dry

diethyl ether was added a suspension of 42 mg (0.374 mmol) of KO^tBu in 15 mL of diethyl ether, and the mixture was stirred for 0.5 h at 0 °C. To the mixture was added 0.09 mL (1.24 mmol) of ethyl iodide and the mixture was stirred for 1 h at 0 °C, and then overnight at room temperature. The mixture was washed with water and dried over MgSO₄. Column chromatography on silica gel with dichloromethane–hexane (1:3) as the eluent afforded 32 mg (0.082 mmol, 82%) of **2**, mp 266–272 °C (dec) (from dichloromethane–hexane). Found: C, 86.19; H, 6.14; N, 3.77%. Calcd for $C_{28}H_{23}NO$: C, 86.34; H, 5.95; N, 3.60%. 1H NMR ($CDCl_3$) δ 1.259 (3H, t, $J = 7.1$ Hz, CH₃), 4.441 (2H, q, $J = 7.1$ Hz, CH₂), 5.324 (1H, s, 10-H), 6.891 (3H, td, $J = 7.6$, 1.5 Hz, 2/7/14-H), 6.968 (3H, td, $J = 7.3$, 1.3 Hz, 3/6/15-H), 7.18 (1H, m, *p*-H), 7.30 (2H, m, *m*-H), 7.372 (3H, dd, $J = 7.2$, 1.3 Hz, 4/5/16-H), 7.41 (2H, m, *o*-H), 7.543 (3H, dm, $J = 7.6$ Hz, 1/8/13-H). ^{13}C NMR ($CDCl_3$) δ 13.62 (1C, p), 54.62 (1C, t), 68.46 (1C, s), 77.42 (1C, q), 123.05 (3C, t), 124.19 (3C, t), 124.92 (3C, t), 125.28 (1C, t), 125.46 (2C, t), 125.79 (3C, t), 128.21 (2C, t), 144.21 (3C, q), 145.22 (3C, q), 146.70 (1C, q).

X-ray Crystallography. Crystals of compounds **2**, **4**, **6**, **7**, and **8** were grown from dichloromethane–hexane. The crystal data and the parameters for data collection, structure determination, and refinement are summarized in Table 4. Diffraction data were collected on a Rigaku AFC7R or a Rigaku/MS Mercury CCD diffractometer and calculations were performed using the SHELXL97 program.²⁶ The structures were solved by direct methods followed by full-matrix least-squares refinement with all non-hydrogen atoms anisotropic and all hydrogen atoms isotropic. Reflection data with $|I| > 2.0\sigma(I)$ were used. The function minimized was $\Sigma w(|F_o| - |F_c|)^2$, where $w = [\sigma^2(F_o)]^{-1}$.

Crystallographic data of these compounds have been deposited at the CCDC, 12 Union Road, Cambridge, CB2 1EZ, UK and copies can be obtained on request, free of charge, by quoting the publication citation and the deposition numbers 254810–254814.

Table 4. Crystal Data of Compounds **2**, **4**, **6**, **7**, and **8** and Parameters for Data Collection, Structure Determination, and Refinement

Compound	2	4	6	7	8
Empirical formula	$C_{28}H_{23}NO$	$C_{26}H_{19}N$	$C_{27}H_{19}N_3O_3$	$C_{26}H_{18}NO$	$C_{26}H_{17}NO$
Formula weight	389.47	345.45	433.47	360.44	359.43
Crystal system	monoclinic	orthorhombic	monoclinic	monoclinic	monoclinic
Space group	$P2_1/c$	$P2_12_12_1$	$P2_1/a$	$P2_1/n$	$P2_1/a$
$a/\text{\AA}$	14.399(4)	13.446(5)	14.129(5)	9.717(3)	13.694(5)
$b/\text{\AA}$	16.953(5)	15.611(3)	8.025(3)	15.718(4)	8.122(3)
$c/\text{\AA}$	16.788(5)	8.763(2)	18.620(7)	12.023(3)	16.889(6)
$\beta/^\circ$	91.7042(13)	90.00	94.017(7)	93.380(13)	106.687(15)
$V/\text{\AA}^3$	4096.2(19)	1839.4(9)	2106.1(13)	1833.1(8)	1799.3(11)
Z	8	4	4	4	4
$D_c/\text{g cm}^{-3}$	1.263	1.247	1.265	1.306	1.327
$F(000)$	1648	728	796	756	752
$\mu(\text{Mo K}\alpha)/\text{cm}^{-1}$	0.71070	0.71069	0.71070	0.71070	0.71069
Temp/K	113(2)	293(2)	113(2)	110(2)	110(2)
$2\theta_{\text{max}}/^\circ$	55	54.5	55	55	55
No. of reflections measured					
Total	7867	2409	3095	3996	3959
Unique	6900	1637	2890	3566	3440
No. of refinement variables	544	321	304	326	322
Final R ; R_w	0.0525; 0.1384	0.038; 0.082	0.063; 0.167	0.046; 0.121	0.063; 0.156
GOF	1.060	1.072	1.048	1.095	1.202

$$R = \Sigma ||F_o| - |F_c|| / \Sigma |F_o|, R_w \text{ on } F^2.$$

Selected Lengths and Angles of Compound 6. Selected lengths (Å) and angles (°) are as follows (the numberings are shown in Fig. 1). N1–O1: 1.293(3), N1–N2: 1.278(3), N2–N3: 1.333(3), N1–C1: 1.478(3), C1–C2: 1.557(3), C1–C3: 1.547(3), C1–C4: 1.536(4), N3–C5: 1.393(3), C6–O2: 1.211(4), C6–O3: 1.330(4), O1–N1–C1: 118.0(2), O1–N1–N2: 122.3(2), C1–N1–N2: 118.7(2), N1–C1–C2: 117.8(2), N1–C1–C3: 108.6(2), N1–C1–C4: 111.6(2), N1–N2–N3: 112.0(2), N2–N3–C5: 118.7(2), N3–C5–C6: 120.0(2), C5–C6–C7: 120.3(2), C6–C7–O2: 124.9(3), C6–C7–O3: 113.2(3), C1–N1–N2–N3: 172.5(2), O1–N1–N2–N3: 4.5(4), N1–N2–N3–C5: 171.2(2), N2–N1–C1–C2: 20.0(3), N2–N1–C1–C3: –101.2(3), N2–N1–C1–C4: 140.9(2), O1–N1–C1–C2: –171.4(2), O1–N1–C1–C3: 67.4(3), O1–N1–C1–C4: –50.5(3), N2–N3–C5–C6: –168.5(3), N3–C5–C6–C7: –0.2(4), C5–C6–C7–O2: –14.7(5), C5–C6–C7–O3: 164.2(3).

Lineshape Analysis. Total lineshape analysis was performed by visual matching of experimental spectra with theoretical spectra computed on an NEC PC9821Xs personal computer equipped with a Mutoh PP-210 plotter. For the calculations of theoretical spectra, we used the DNMR3K program, a modified version of the DNMR3 program²⁷ converted for use on personal computers by Dr. Hiroshi Kihara. Temperature dependences of chemical shift differences and T_2 values were properly taken into account.

Saturation Transfer Experiments on 8. In the study of the Tp–N rotation, the 1,8-H signal at δ 6.88 was saturated by irradiation of a high-frequency field and the 13-H signal at δ 8.12 was monitored. The change in the signal intensity, $I(t)$, was followed as a function of the duration of the irradiation, t , over the range of 1 ms to 8 s. The data were fitted to the exponential function (Eq. 1) and the three coefficients, A , B , and C , were determined by nonlinear least squares analysis.²⁸

$$\frac{I(t)}{I(0)} = A + B \exp(-Ct) \quad (1)$$

$$\text{where } A = \frac{\tau_1}{T_1}, \quad B = \frac{\tau_1}{\tau}, \quad C = \frac{1}{\tau_1} = \frac{1}{\tau} + \frac{1}{T_1}.$$

Here T_1 and τ are the spin–lattice relaxation time and the lifetime, respectively, of the 13-H signal. The rate constant for the Tp–N rotation is given by $1/(2\tau)$, because $1/\tau$ corresponds to the sum of two rate constants, $k(13\text{-H} \rightarrow 1\text{-H})$ and $k(13\text{-H} \rightarrow 8\text{-H})$, and the rate constant for the Tp–N rotation corresponds to one of them.

Similarly, the rate constants for the C=N bond topomerization were obtained by following the change in the signal intensity of H^P (δ 7.81) upon irradiation of H^B (δ 6.57). Here the topomerization rate constant is given by $1/\tau$.

We thank Professor Hideyo Matsuzawa of Kitasato University for obtaining the ESR spectrum of compound 7.

References

- G. Yamamoto, H. Higuchi, M. Yonebayashi, and J. Ojima, *Chem. Lett.*, **1994**, 1911.
- G. Yamamoto, H. Higuchi, M. Yonebayashi, Y. Nabeta, and J. Ojima, *Tetrahedron*, **52**, 12409 (1996).
- G. Yamamoto, H. Higuchi, M. Yonebayashi, Y. Nabeta, and J. Ojima, *Chem. Lett.*, **1995**, 853.
- G. Yamamoto, K. Inoue, H. Higuchi, M. Yonebayashi, Y. Nabeta, and J. Ojima, *Bull. Chem. Soc. Jpn.*, **71**, 1241 (1998).
- G. Yamamoto, H. Murakami, N. Tsubai, and M. Mazaki, *Chem. Lett.*, **1997**, 605.
- G. Yamamoto, N. Tsubai, H. Murakami, and M. Mazaki, *Chem. Lett.*, **1997**, 1295.
- G. Yamamoto, F. Nakajo, N. Tsubai, H. Murakami, and M. Mazaki, *Bull. Chem. Soc. Jpn.*, **72**, 2315 (1999).
- G. Yamamoto, F. Nakajo, and M. Mazaki, *Bull. Chem. Soc. Jpn.*, **74**, 1973 (2001).
- G. Yamamoto, K. Kuwahara, and K. Inoue, *Chem. Lett.*, **1995**, 351.
- G. Yamamoto, C. Agawa, and M. Minoura, *Bull. Chem. Soc. Jpn.*, **76**, 825 (2003).
- G. Yamamoto, F. Nakajo, N. Endo, and M. Mazaki, *Chem. Lett.*, **2000**, 1102.
- G. Yamamoto, F. Nakajo, N. Endo, and M. Mazaki, *Bull. Chem. Soc. Jpn.*, **74**, 1467 (2001).
- F. M. Logullo, A. H. Seitz, and L. Friedman, *Org. Synth.*, Coll. Vol. **V**, 54 (1973).
- T. C. Bissot, R. W. Parry, and D. H. Campbell, *J. Am. Chem. Soc.*, **79**, 796 (1957).
- D. H. Everett and W. F. K. Wynne-Jones, *Proc. R. Soc. London*, **A177**, 499 (1941).
- A. K. Majumdar and S. C. Saha, *Anal. Chim. Acta*, **40**, 299 (1968).
- S. B. Sarkar, M. Khalil, S. C. Saha, and S. K. Talapatra, *Acta Crystallogr.*, **C39**, 1075 (1983).
- H. Kaur, M. J. Perkins, A. Scheffer, and D. C. Vennor-Morris, *Can. J. Chem.*, **60**, 1594 (1982).
- J. Ohshita, T. Iida, N. Ohta, K. Komaguchi, M. Shiotani, and A. Kunai, *Org. Lett.*, **4**, 403 (2002).
- N. Benfaremo, M. Steenbock, M. Klapper, K. Müllen, V. Enkelmann, and K. Cabrera, *Liebigs Ann. Chem.*, **1996**, 1413.
- W. B. Jennings and V. E. Wilson, "Acyclic Organonitrogen Stereodynamics," ed by J. B. Lambert and Y. Takeuchi, VCH, New York (1992), Chap. 6; H. O. Kalinowski and H. Kessler, *Top. Stereochem.*, **7**, 295 (1973); A. P. Avedeenko, *Russ. J. Org. Chem.*, **36**, 522 (2000).
- W. B. Jennings and D. R. Boyd, *J. Am. Chem. Soc.*, **94**, 7187 (1972).
- A. Rieker and H. Kessler, *Tetrahedron*, **23**, 3723 (1967).
- G. Yamamoto and M. Ōki, *Bull. Chem. Soc. Jpn.*, **57**, 2219 (1984).
- W. Theilacker and K.-H. Beyer, *Chem. Ber.*, **94**, 2968 (1961).
- G. M. Sheldrick, "Program for the Refinement of Crystal Structures," University of Göttingen, Germany (1997).
- D. A. Kleier and G. Binsch, QCPE Program No. 165.
- S. Forsén and R. A. Hofmann, *J. Chem. Phys.*, **39**, 2892 (1963); J. Sandström, "Dynamic NMR Spectroscopy," Academic Press, London (1982), Chap. 4.